Observations, data acquision, data analysis: Transit Photometry

Avidaan Srivastava

1 Introduction

Transit photometry is one of the methods use to look for planets orbiting stars beyond our solar system. As of yet, the majority of exoplanets discovered (4060) have been via transits. The main contributor to these detections was NASA's Kepler satellite that remained operational from 2009 to 2018. Some other prominent telescopes that are involved in detection of exoplanet via this method are the Transiting Exoplanet Survey Satellite and Wide Angle Search for Planets.

The basic principle of transit photometry involves the counting of photons receive from the target star for a significant duration of time. When a planet orbiting a star appears in our line of side to said star, it blocks a portion of the star's incoming light (Figure 1) which we can measure in the form of the change in the flux (brightness) observed by our instrument. This change in flux with time is called a lighturve which can help in inferring various properties of the planet such as its radius (Equation 1), equilibrium temperature (Equation 2) and the semi-major axis (Equation 3).

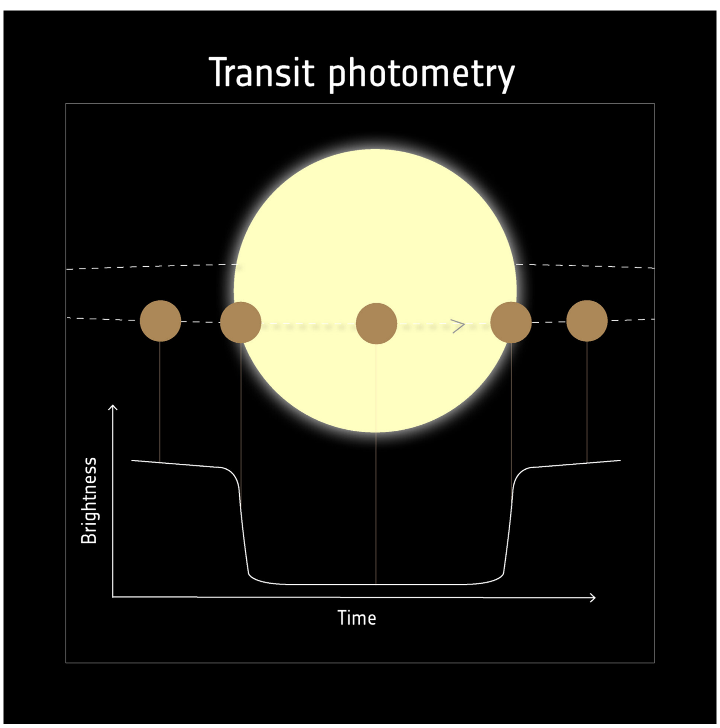

Figure 1: Principle of transit photometry (ESA)

$$\delta F = \left(\frac{R_{planet}}{R_{star}}\right)^2 \tag{1}$$

$$T_{eq} = T_{star}\left(\frac{R_{star}}{2a}\right)^{1/2} \tag{2}$$

$$a = R_{star}\,\frac{2P}{\pi}\frac{\delta F^{1/4}}{(t_T^2 - t_F^2)^{1/2}} \tag{3}$$

Here, δF refers to the transit depth (drop in stellar brightness during transit), R_{star} and R_{planet} refer to the stellar and planetary radii respectively, T_{eq} is the equilibrium temperature of the planet, T_{star} is the effective temperature of the star, a represents the semi-major axis of the star-planet system and finally t_T is the total transit duration and t_F is the transit duration only when the planet is fully occulted by the star.

The goal of this module is to construct the transit lightcurve of WASP-49 using the raw images taken via EulerCam (4k x 4k CCD) located on the 1.2-m Swiss Euler Telescope in Chile. The data was taken on 18^{th} February 2021.

2 Methods

The key components needed for this module are: a working version of python and a FITS image viewer, SAO DS9 here. The images taken by ECAM fell into one of three categories:

- Flat field: Images of an evenly illuminated area, used to map out the detector's sensitivity variations
- Bias: Images taken with an exposure time of 0-seconds, used to determine the 0-level of the detector
- Science frames: Raw images that need to be corrected for instrumental effects and then used for science

The flat field and bias images are used for calibrations and together with the raw science images produce the reduced science images that can finally be used for aperture photometry.

2.1 Image Correction

Expanding on previously mentioned image reduction, the first step to achieving that is by creating a *masterbias* frame. This is done by creating a per pixel average of all the 9 bias images. This *masterbias* is then subtracted from each of the 5 flat field images. The new flat field images are then averaged and normalized with respect to a 1000x1000 pixel region in the center to produce the *normflat*. Equation 4 shows a relation to convert the 69 raw images to the final reduced science images. Additionally, 100 pixels from each edge are removed to exclude the image borders. Figure 2 shows one of the final reduced images.

$$reduced\,image = \frac{raw\,image\, -\, masterbias}{normflat} \tag{4}$$

2.2 Aperture Photometry

The concept of *Aperture Photometry* involves first locating the target star on the image and cropping a 200 x 200 pixel *subimage* around it. Figure 3 shows one such subimage of WASP-49. Here the red circle acts as an aperture that contains the majority of the light from the star. The area within the two yellow circles will be used to measure the background flux. The radii of all these circles depends on the point

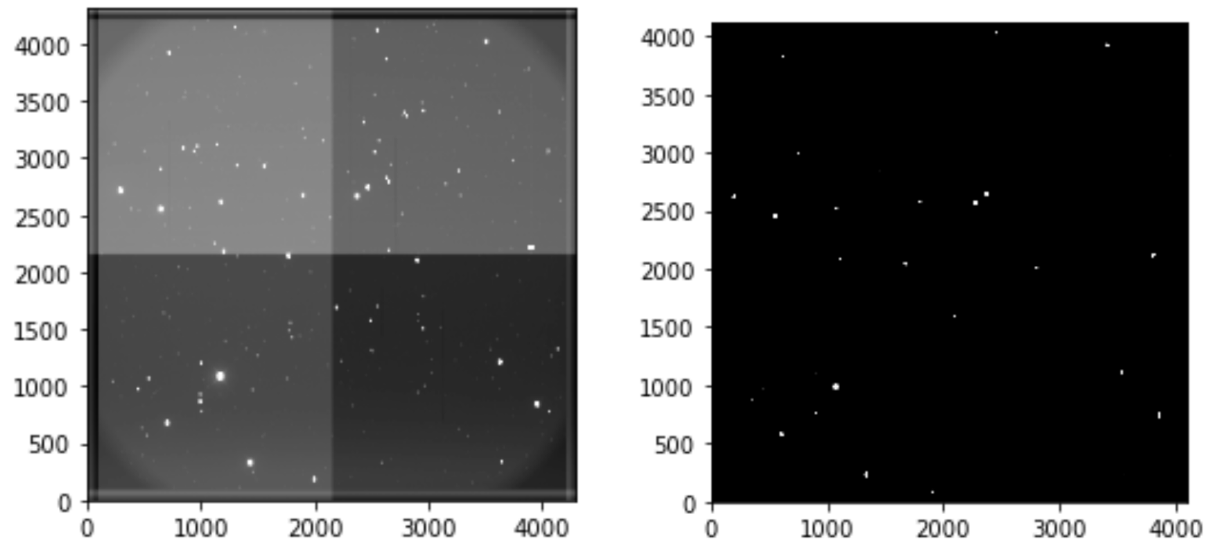

(a) Original Image

(b) Reduced Science Image

Figure 2: Comparing the same image before and after reduction

spread function (PSF) of the target star with a good enough guess for the yellow annulus' location such that it is far away from any bright stars on the image.

To make this process slightly more organized and accurate, the centroid of the subimage is first calculated, weighted by the flux in each pixel. Equation 5 shows the relation needed to obtain the coordinates of the centroid. The next step is to determine the a reasonable radius for the aperture. One way to do so is to plot the flux within the aperture as a function of the aperture width as shown in Figure 4. Here, an aperture size of 35 pixels is deemed sufficient as the increase in flux is insignificant if the aperture size is increased further. Similarly, for the background, the inner and outer radii are 85 and 95 pixels respectively. The flux is then set to 0 at all points outside of the aperture and the subimage flux inside the annulus is then subtracted by the background flux, resulting in a new subimage as shown in Figure 3.

$$cx = \frac{\Sigma_x \left(x\, \Sigma_y\, F_{x,y}\right)}{\Sigma_x\, \Sigma_y \left(F_{x,y}\right)} \;\; ; \;\; cy = \frac{\Sigma_y \left(y\, \Sigma_x\, F_{x,y}\right)}{\Sigma_x\, \Sigma_y \left(F_{x,y}\right)} \tag{5}$$

2.3 Time-series Photometry

Building up on the work done in the previous section, the process is repeated for all 69 reduced science images. However, photometry relies solely on counting the photons entering the detector which is why a reference point is needed in order to get a normalized value for the target star's flux. To accomplish this, the aperture photometry process is repeated for another star on the image, preferably keeping the aperture size and background annulus size the same for consistency. Multiple reference stars can be used to optimize the normalization but here only one was used.

All 69 images were taken at different timestamps and therefore a timeseries of subimages is obtained containing the measurement of the flux from the target and reference stars inside the apertures as a function of time. The *flux array* of WASP-49 is then divided by that of the reference star to get the normalized flux. The total normalized flux for each timestamp is plotted in Figure 5, giving the final lightcurve. The flux values of points highlighted in orange are averaged out to infer the transit depth of

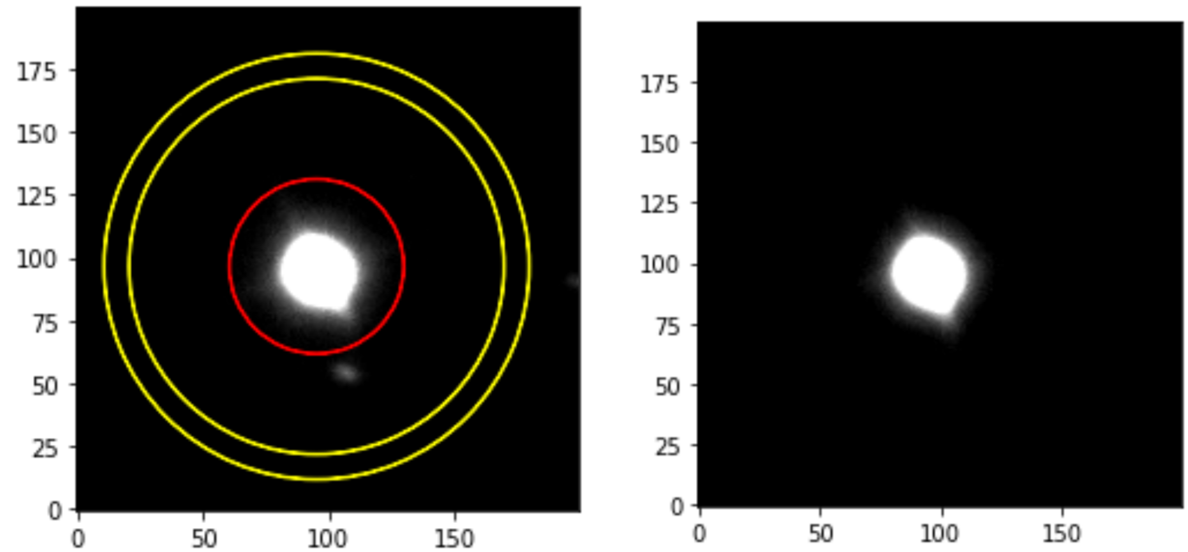

(a) WASP-42 with aperture ring (red) and background annulus (yellow)

(b) WASP-42 after isolating aperture flux and subtracting background

Figure 3: Aperture photometry of WASP-42

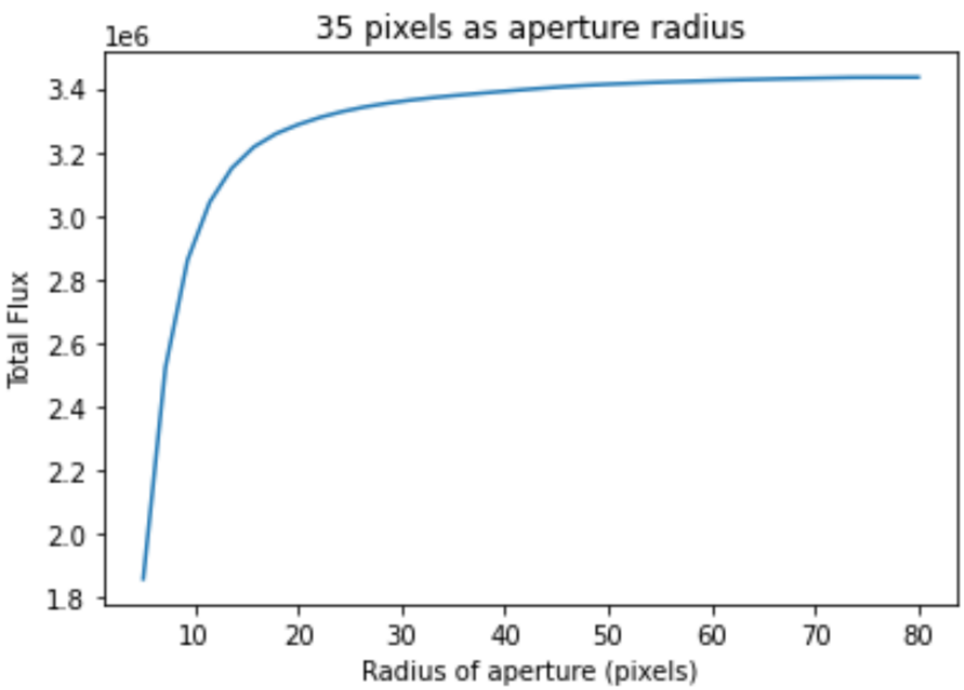

Figure 4: Flux inside the aperture as a function of aperture size

1.26%. Estimating from the lightcurve, t_F lasts from 0.082 to 0.14 (+2459263e6) days and t_T from 0.07 to 0.152 (+2459263e6) days.

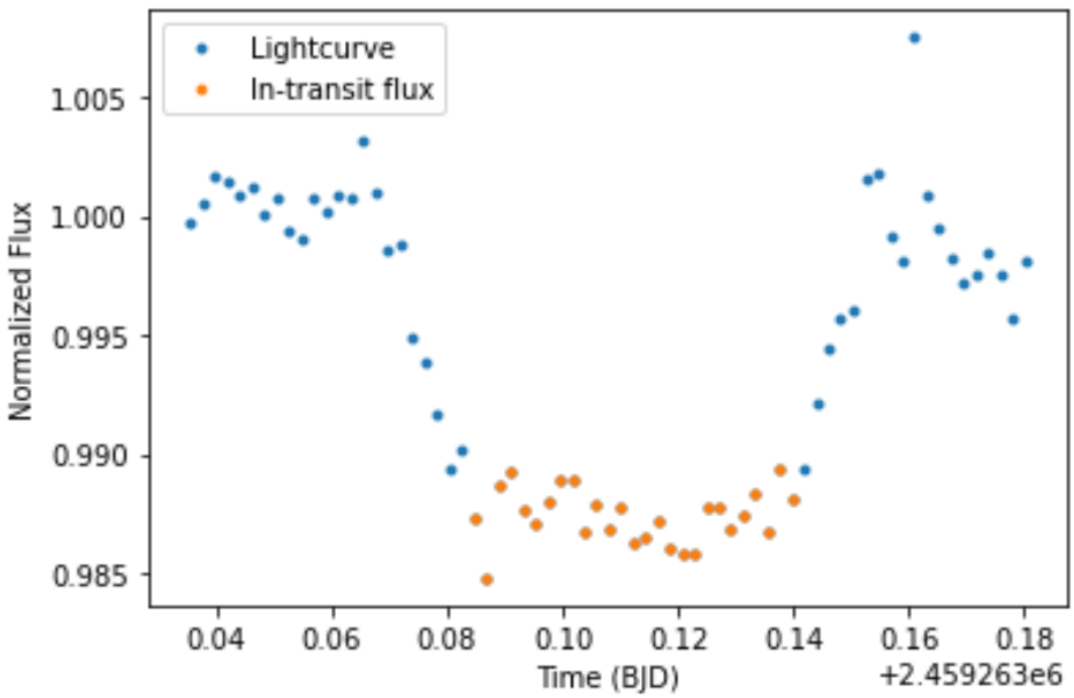

Figure 5: Lightcurve of WASP-42 showing the signature of WASp-42b

3 Results

Based on equations mentioned previously, the following quantities were recovered about the planet using supplementary stellar parameters listed in the module documentation.

- $R_{planet} = 1.0063 \pm 0.123\, R_{Jupiter}$
- $T_{eq} = 1238.075\, K$
- $a = 0.0428\, AU$

Comparing these values to the ones listed on NASA's Exoplanet Archive (NEA), the radius of WASP-42b is listed as $1.11 \pm 0.11\, R_{Jupiter}$[2], $a = 0.0379^{+0.0010}_{0.0011}\, AU$[1] and $T_{eq} = 1400 \pm 80\, K$[3]. Although there are some discrepencies in the values, which may have arised due to primarily two reasons: insufficient datapoints or unoptimized flux normalization, to the first approximation they do match with the ones calculated in this module.

References

[1] A. S. Bonomo et al. "The GAPS Programme with HARPS-N at TNG . XIV. Investigating giant planet migration history via improved eccentricity and mass determination for 231 transiting planets". In: 602, A107 (June 2017), A107. DOI: 10.1051/0004-6361/201629882. arXiv: 1704.00373 [astro-ph.EP].

[2] Keivan G. Stassun, Karen A. Collins, and B. Scott Gaudi. "Accurate Empirical Radii and Masses of Planets and Their Host Stars with Gaia Parallaxes". In: 153.3, 136 (Mar. 2017), p. 136. DOI: 10.3847/1538-3881/aa5df3. arXiv: 1609.04389 [astro-ph.EP].

[3] A. Wyttenbach et al. "Hot Exoplanet Atmospheres Resolved with Transit Spectroscopy (HEARTS). I. Detection of hot neutral sodium at high altitudes on WASP-49b". In: 602, A36 (June 2017), A36. DOI: 10.1051/0004-6361/201630063. arXiv: 1702.00448 [astro-ph.EP].